CEPR PRESS

Covid Economics **Issue 18, 15 May 2020**

Lifting restrictions with changing mobility and the importance of soft containment measures: A SEIRD model of COVID-19 dynamics

Salvatore Lattanzio[1] and Dario Palumbo[2]

Date submitted: 11 May 2020; **Date accepted:** 12 May 2020

This paper estimates a SEIRD (susceptible-exposed-infected-recovered-deaths) epidemic model of COVID-19, which accounts for both observed and unobserved states and endogenous mobility changes induced by lockdown policies. The model is estimated on Lombardy and London – two regions that had among the worst outbreaks of the disease in the world – and used to predict the evolution of the epidemic under different policies. We show that policies targeted also at mitigating the probability of contagion are more effective in containing the spread of the disease, than the one aimed at just gradually reducing the mobility restrictions. In particular, we show that if the probability of contagion is decreased between 20% and 40% of its original level before the outbreak, while increasing mobility, the total death toll would not be higher than in a permanent lockdown scenario. On the other hand, neglecting such policies could increase the risk of a second epidemic peak even while lifting lockdown measures at later dates. This highlights the importance during the containment of the disease of promoting "soft" policy measures that could reduce the probability of contagion, such as, wearing masks and social distancing.

1 PhD Candidate, University of Cambridge.
2 Research Fellow, Ca' Foscari University of Venice, University of Cambridge.

Covid Economics 18, 15 May 2020: 1-41

Covid Economics 18, 15 May 2020: 1-41

1 Introduction

The novel coronavirus disease (COVID-19) spread quickly around the world. Many governments have adopted draconian measures to weaken its transmission among the population and some were more successful than others in containing its spread. The adoption of lockdown measures was deemed as necessary when policymakers realized that the virus was more infectious than initially thought, which brought many healthcare systems at the peak of the epidemic contagion to be under serious pressure. At some point the pressure on hospitals, and in particular on intensive care units, was so high that in some cases not all patients were treated. As a consequence, some people died without being diagnosed the infection and they did not enter the official death count. This implies that, in many countries, the official death toll considerably underestimates the true number of deaths (Villa, 2020b). This happens in addition to under-reporting of cases in official statistics. One clear example of the under-reporting of both cases and deaths is Lombardy, the region in Northern Italy where the first cases of COVID-19 appeared in late February. Lombardy is by far the most severely hit region in Italy: as of May 2, with more than 14,000 deaths, it represents 49.4% of the Italian total death toll. In some provinces, though, the true death count is at least twice the official figure, reflecting the difficulties of the healthcare system to cope with the exponential spread of the disease and of intensive care units in admitting all patients that needed medical care, as highlighted also in the media (Cancelli and Foresti, 2020). At the same time, many deaths happened in residential care homes, where many patients were not tested and, therefore, their death was not counted as COVID-19 related. The under-reporting of deaths is evident when comparing official COVID-19 death toll with death registries, available from the Italian Statistical Institute (Istat).[1] Figure 1 reports in panel (a) the daily number of "excess" deaths, defined as the difference between total deaths in 2020 relative to the average of the past 5 years, and the official coronavirus daily deaths in Lombardy in the first 3 months of 2020. To compute excess deaths, the figure uses data for a sample of municipalities in Lombardy that covers approximately 95% of the municipalities in the region and shows that, before the onset of the disease, the number of deaths in 2020 was in line – if not smaller – than the average of previous years. The series increases sharply at the end of February, when the first cases of coronavirus were registered in the region. The official death count is lower than the true number of deaths at all dates, highlighting a downward bias in official death counts. Panel (b) of the figure shows the same pattern for England and Wales, where the excess deaths are computed with the Office for National Statistics (ONS) data and COVID-related deaths are from two sources: ONS and Public Health England. The graph shows a pattern similar to Lombardy, where not all the excess mortality in 2020 is due to COVID-19. Part of this is due to under-reporting, but a part of it may also be due

[1] https://www.istat.it/it/archivio/240401

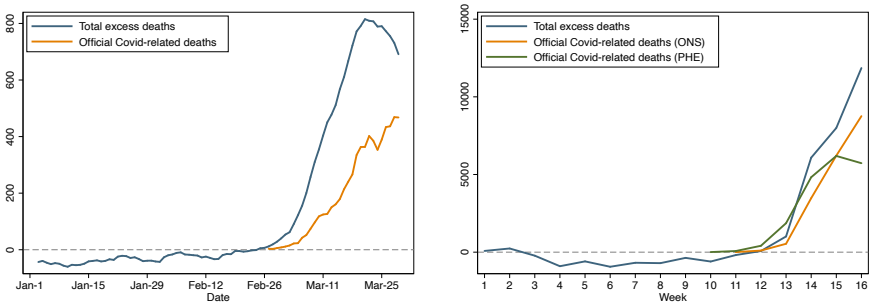

(a) Lombardy (b) England and Wales

Figure 1: Excess deaths in 2020 and official COVID-19 deaths

Notes. The figure shows excess mortality in 2020 relative to the average of previous 5 years and COVID-19 official deaths. Panel (a) reports daily data for Lombardy (averaged over a 5-day rolling window), where excess deaths are computed over a sample that comprises 95% of the municipalities in the region, whereas panel (b) reports data for England and Wales. Data: Istat, Protezione Civile, Office for National Statistics, Public Health England.

Covid Economics 18, 15 May 2020: 1-41

to deaths not directly related to coronavirus, but indirectly linked to it, if patients with other pathologies do not receive appropriate treatment because of overwhelmed hospitals.

This evidence suggests that, when trying to model the evolution of the disease, it is of utmost importance to take into account both observed and unobserved infection and death counts. This paper aims at doing so, by developing a compartmental susceptible-exposed-infected-recovered-deaths (SEIRD) model with two main compartments – observed and unobserved – of infections, recoveries and deaths, extending the classic SIR model first introduced by Kermack and McKendrick (1927). The model is estimated with Kalman filter techniques and used to forecast the evolution of the epidemic under a number of different scenarios. We calibrate the model on official data for Lombardy and London. In fact, the United Kingdom experienced an evolution of the epidemic similar to Italy and London, in particular, accounts for the majority of deaths in the country (approximately 25% of the official death toll).

Our model accounts for the underestimation of true cases, by calibrating the under-reporting intensity to time-series obtained by correcting the observed case fatality rate with the infection fatality rate estimated in the literature (Ferguson et al., 2020; Villa, 2020a). Moreover, it accounts for the under-estimation of total deaths by explicitly modeling observed and unobserved deaths and calibrating the true mortality rate to be proportional to the number of excess deaths recovered from death registries. Finally, we account for mobility restrictions in the estimation of the infection probability, one key parameter that governs the rate at which susceptible individuals get exposed to the disease. We use mobility trends in Lombardy from Pepe et al. (2020) and in London from Google Community Mobility Reports and estimate the initial contact rate, given the rate of change of mobility. Therefore, we explicitly model lockdown by accounting for the decrease in

mobility of individuals after its imposition.

Our model suggests that at the end of the fit period used to estimate the parameters (9 April in Lombardy, 15 April in London), the prevalence of the disease is approximately 5.7% in Lombardy and 2% in London. The number of unobserved infected cases is at least twice as large as observed cases in both regions, whereas the number of unobserved recoveries is between 20 and 26 times larger than observed recoveries. The true death count is underestimated by 35% in Lombardy and 17% in London.

We use our model to forecast the evolution of the disease under different policy scenarios. Specifically, we consider a number of policy measures that go from lifting immediately all lockdown measures to maintaining them until mid-summer, with different intermediate scenarios, where restrictions are gradually lifted over time. Our forecasts suggest that with appropriate measures that reduce the probability of contagion by 20% to 40% of its pre-lockdown level, lifting restrictions would not entail a second epidemic peak, even in the presence of increased mobility, both in Lombardy and London. In other terms, with appropriate policies that reduce the probability an individual is infected – e.g. social distancing, using masks, increasing hygiene standards, isolating infected cases –, we show that gradually and carefully lifting lockdown measures does not imply a resurgence of the epidemic curve. This result may provide guidance to policymakers when deciding how and when lifting lockdowns. Our model suggests that the trade-off between economic recovery and saving lives can be balanced by implementing soft containment measures that could reduce the spread of the virus, even in the presence of increased mobility.

The rest of the paper is organized as follows. Section 2 details the methodology for modeling the evolution of the pandemic. Section 3 details the estimation results. Section 4 provides model forecasts and the predictions about policy counterfactuals. Finally, section 5 concludes.

2 Methodology

We base our modeling on a susceptible-exposed-infected-recovered-deaths (SEIRD) model with two compartments – detected or observed and undetected or unobserved – of infected, recovered and deaths. From the beginning of the epidemic, many researchers have highlighted the severe under-reporting of cases in official statistics. As tests are conducted on symptomatic individuals only, there is a large fraction of asymptomatic and mildly sympomatic cases that are not reported in official statistics (Lavezzo et al., 2020; Li et al., 2020a; Russo et al., 2020). Moreover, the stress on hospitals has led to a severe underestimation of deaths, too (Bucci et al., 2020). For this reason we augment the classic SIR model (Kermack and McKendrick, 1927), by accounting for both observed and unobserved states.

SIR models have been used extensively in the modeling of the COVID-19 spread

Covid Economics 18, 15 May 2020: 1-41

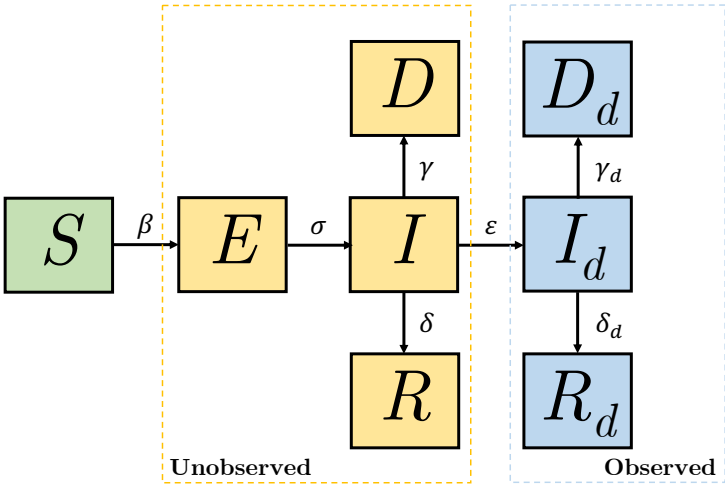

Figure 2: SEIRD model with unobserved and observed compartments

(Favero, 2020; Giordano et al., 2020; Russo et al., 2020; Toda, 2020; Toxvaerd, 2020). The version here proposed assumes the existence of 8 states, summarized in Figure 2: susceptible S_t, exposed E_t, infected unobserved I_t, infected observed I_{dt}, recovered unobserved R_t, recovered observed R_{dt}, deaths unobserved D_t and deaths observed D_{dt}. Every individual in the population at every point in time belongs to one of these categories. The discrete dynamics of the system are described as follows,

$$
\begin{aligned}
S_t &= \left(1 - \frac{\beta}{N - D_{t-1} - D_{dt-1}} I_{t-1}\right) S_{t-1} \\
E_t &= (1-\sigma)\, E_{t-1} + \frac{\beta}{N - D_{t-1} - D_{dt-1}} S_{t-1} I_{t-1} \\
I_t &= (1 - \delta - \epsilon - \gamma)\, I_{t-1} + \sigma E_{t-1} \\
I_{dt} &= (1 - \delta_d - \gamma_d)\, I_{dt-1} + \epsilon I_{t-1} \\
R_t &= R_{t-1} + \delta I_{t-1} \\
R_{dt} &= R_{dt-1} + \delta_d I_{dt-1} \\
D_t &= D_{t-1} + \gamma I_{t-1} \\
D_{dt} &= D_{dt-1} + \gamma_d I_{dt-1}
\end{aligned}
$$

where N is total size of the population,[2] β, σ, ϵ, δ, δ_d, γ, γ_d are the static parameters which determine the transitions between the states in the dynamics. In particular, we have that all parameters are strictly positive, then $0 < \sigma < 1$, $0 < \delta + \epsilon + \gamma < 1$ and

[2]We do not allow for variations in population size which might have occurred in the time periods considered. For the purpose of our study we assume them to be marginal in respect to total population.

$0 < \delta_d + \gamma_d < 1$. The subscript d indicates detected variables or parameters referred to detected variables.

Given that the observed variables are only $\mathbf{y}_t = (I_{dt}, R_{dt}, D_{dt})'$ and are observed with noise, we can represent this dynamic system with a non-linear state space

$$\begin{aligned} \mathbf{y}_t &= \mathbf{Z}\boldsymbol{\alpha}_t + \boldsymbol{\varepsilon}_t & \boldsymbol{\varepsilon}_t &\sim N(\mathbf{0}, \Omega_\varepsilon) \\ \boldsymbol{\alpha}_t &= \mathbf{T}(\boldsymbol{\alpha}_{t-1}) + \boldsymbol{\eta}_t & \boldsymbol{\eta}_t &\sim N(\mathbf{0}, \Omega_\eta) \end{aligned}$$

where $\boldsymbol{\alpha}_t = (S_t, E_t, I_t, I_{dt}, R_t, R_{dt}, D_t, D_{dt})'$ is the unobserved state vector, $\mathbf{Z}$ is the time invariant matrix

$$\mathbf{Z} = \begin{pmatrix} 0 & 0 & 0 & 1 & 0 & 0 & 0 & 0 \\ 0 & 0 & 0 & 0 & 0 & 1 & 0 & 0 \\ 0 & 0 & 0 & 0 & 0 & 0 & 0 & 1 \end{pmatrix}$$

and $\mathbf{T}(.)$ is the multivariate function describing the linear and non-linear relations between the state vector relating $t-1$ and t. Following Harvey (1989), the estimation of the sequence $(\boldsymbol{\alpha}_t)_{t=1}^T$ is obtained through an Extended Kalman Filter, and the estimation of the unknown parameters by maximizing the likelihood obtained by the resulting prediction error decomposition.[3]

As showed by Diekmann et al. (1990) and Heffernan et al. (2005), the basic reproductive ratio (R_0) for continuous time SEIR compartmental epidemic models is defined as the dominant eigenvalue of the "next generation operator," which is the matrix that describes the rates at which infected individuals in one infected state can produce new infected individuals from another state, times the average length of time period that an infected individual spends in her own compartment. In a state-space SIR model Kucinskas (2020) shows that it can be identified from the daily growth rate in the number of infected individuals at time 0. On the other hand, Tibayrenc (2007) shows it can be approximated by $R_0 = \beta\tau$, where τ is the duration of the infectivity. Following Diekmann et al. (1990) the R_0 of our model reads as[4]

$$R_0 = \frac{\beta}{\epsilon + \delta + \gamma} \tag{1}$$

This result coincides with Russo et al. (2020) where R_0 is obtained from the necessary condition for convergence on the Jacobian matrix of the subsystem of the three infected states E_t, I_t, I_{dt}.

For the model to be valid we need that at each time t the sum of all the states is equal to N. In order to impose this restriction while using the Kalman Filter we follow the

[3]For details on the state equation specification under the Extended Kalman Filter see Appendix A.
[4]For the details on the derivation see Appendix B.

Covid Economics 18, 15 May 2020: 1-41

approach of Doran (1992) and augment the cross-section of each observation vector $\mathbf{y}_t$ of an additional observation set constant as N for every t. Then the transition equation for this series becomes $\sum_j \alpha_{jt} = N$ at every t. While assuming that this additional series has a Gaussian uncorrelated measurement error with $E[\varepsilon_{0t}] = 0$ and $E[\varepsilon_{0t}^2] = 0$, the constraint is guaranteed to hold in both the updating and smoothing equations of the Kalman Filter.

3 Calibration and Estimation

3.1 Data and Initial Conditions

The current study is based on the COVID-19 contagion data for Lombardy and London. The data for Lombardy are obtained from the Github repository of Protezione Civile Italiana.[5] We collect daily data on the current total number of COVID-19 infected positively tested, number of recovered and total number of COVID-19 deaths in the region from 24/02/2020 to 09/04/2020. The data provided by Protezione Civile are reported before being confirmed by the Italian National Institute of Health (ISS). Due to this delay there might be reporting differences with the actual number of detected individual and this certainly is one of the contributors to the noise in the measurment of the true detected variables.

In regards to London, we have collected daily data on the total number of COVID-19 infected from the UK Government COVID-19 data dashboard[6] and on the total number of COVID-19 hospital deaths from the NHS website[7] from 01/03/2020 to 17/04/2020. The data on recovered patients are not publicly available for the London area, and the total number of infected TI_{dt} is now a sum of I_{dt}, R_{dt} and D_{dt}. Therefore in the case of London we modify the transition equation for an observed vector of $\mathbf{y}_t = (TI_{dt}, D_{dt})'$ where $\mathbf{Z}$ is now redefined as

$$\mathbf{Z}_{Lon} = \begin{pmatrix} 0 & 0 & 0 & 1 & 0 & 1 & 0 & 1 \\ 0 & 0 & 0 & 0 & 0 & 0 & 0 & 1 \end{pmatrix}$$

In estimating the model on the two datasets, we set the total population in the two regions equal to $N_{Lom} = 10,060,574$ for Lombardy,[8] and $N_{Lon} = 9,050,506$ for London.[9]

To partly solve the identification problem we assume that there is no correlation in the cross-section between the disturbances of the state equation and that they are homoschedastic, i.e. $\Omega_\eta = \sigma_\eta^2 \mathbf{I}$. On the other hand, measurement errors in the transition

[5] https://github.com/pcm-dpc/COVID-19
[6] https://coronavirus.data.gov.uk
[7] NHS, COVID-19 Daily Deaths.
[8] Istat, Resident population on the 1st of January, 2019.
[9] ONS, Subnational population projections, 2018.

Covid Economics 18, 15 May 2020: 1-41

equation can be due to different sources. Therefore, while we still assume no correlation in the cross-section, we assume that the variances are heteroschedastic

$$\Omega_{\varepsilon Lom} = \begin{pmatrix} \sigma^2_{1\varepsilon} & 0 & 0 \\ 0 & \sigma^2_{2\varepsilon} & 0 \\ 0 & 0 & \sigma^2_{3\varepsilon} \end{pmatrix} \qquad \Omega_{\varepsilon Lon} = \begin{pmatrix} \sigma^2_{1\varepsilon} & 0 \\ 0 & \sigma^2_{2\varepsilon} \end{pmatrix}$$

In SEIR models the initial conditions imply that all states should equal 0 at $t = 0$. In our specification we assume that $S_0 = N$. However, given that in both settings data on COVID-19 infections begin to be reported after the outbreak has already started, we cannot have initial states starting at 0. For this reason, we set I_{d0}, R_{d0}, D_{d0} at their values at the beginning of the datasets. Among the remaining state variables we set $D_0 = Y_{d0} \times 0.015$ and we estimate the other initial conditions, imposing that $S_0 > E_0 > I_0 > I_{d0} > R_0$ and that $\sum_j \boldsymbol{\alpha}_{j0} = N$. Finally, the standard errors of the estimated parameters are computed by bootstrap following Stoffer and Wall (1991).

3.2 Parameter Description

The introduced SEIRD model has 8 time-invariant parameters which describe the evolution of the disease over time, β, σ, ϵ, δ, δ_d, γ, γ_d. The estimation of all the parameters, including the elements of the covariance matrices Ω_ϑ and Ω_η, creates an issue of identification. We address this problem by calibrating some of the parameters.[10]

σ is the rate at which the exposed individuals become infected. This is usually set equal to the inverse of the incubation period of the disease. Li et al. (2020b) collected data on the first 425 confirmed cases in Wuhan and found that the median incubation period was 5.2 days with 95% confidence intervals between 4.1 and 7 days. These results are also also consistent with the findings of Lauer et al. (2020). Another study by Li et al. (2020a) assessed the prevalence of the novel coronavirus for the reported cases in China with a Bayesian Networked Dynamic Metapopulation Model with data on mobility. The study estimates the fraction of undocumented infections and their contagiousness finding a mean latency period in the transmission of the disease of 3.42 days with 95% confidence intervals between 3.30 and 3.65 days. We have estimated our model on the samples selected for a range of values of $1/\sigma$ between $[3, 7]$ finding that the estimates of β, and as a consequence R_0, where practically unchanged. We ultimately set $1/\sigma = 3$, using the lower bound of the range.

ϵ, δ and γ are, respectively, the proportion of the infected unobserved I_t which become detected, recovered, and die at each time period t. According to the guidelines of the

[10] As highlighted by Russo et al. (2020), the actual transition of the individuals across these states is reported with a time delay. Therefore these parameters are not exactly the average daily transition rates.

Covid Economics 18, 15 May 2020: 1-41

WHO, a normal flu should go away between a week or two.[11] Symptoms of fever should disappear between 4 to 5 days but cough might still be present. On the other hand, according to Day (2020), from the data available from Wuhan we also have that 4 out 5 cases are asymptomatic. For these reason we calibrate the average recovery period to 5 days resulting in a $\delta = 1/5$.

δ_d and γ_d are the proportions of the infected observed I_{dt} which recover or ultimately die, respectively. Among detected infected, few of the individuals are positively tested with mild symptoms and home-isolate, whereas the majority are those with severe symptoms who are hospitalized. According to a recent WHO report, patients with severe or critical symptoms take between 3 to 6 weeks to recover (WHO, 2020). In light of this, we assume the recovery time for detected infected to be the lower bound of this range. Therefore we set $\delta_d = 1/21$.

3.3 Including Mobility Data

In SEIR models the parameter β describes the infection rate of susceptible individuals, or the "effective" daily transmission rate of the disease. The possibility of temporal heterogeneity in the transmission rate has been extensively studied in the literature to explain the amplitude in the variation in the outbreaks of diseases, from Soper (1929) to Grassly and Fraser (2006). In our context the possible variation in the transmission rate of COVID-19 is mainly related to changes in mobility of the population. The impact of mobility on the transmission rate can be appreciated given its approximate decomposition in the product $\beta \approx \bar{n} p_c$, where $\bar{n}$ is the daily average number of contacts that an individual has in the population and p_c is the actual probability of contracting the disease in a single contact. Alteration in p_c can be due to many factors, among which how each individual actively take precautions to prevent the contagion in each contact. Della Valle et al. (2007), among others, estimates $\bar{n}$ at a given point in time and taking into account heterogeneity between age groups and lifestyles. However, rather than estimating a single value for $\bar{n}$, we are mostly interested in observing its variation over time, which crucially depends on individuals' mobility.

To measure mobility changes during the COVID-19 outbreak, we use data from the Google Community Mobility Reports[12] for London, and from Pepe et al. (2020) for Lombardy. Google reports collect information from smartphones of Google users who opted-in for their location history in their Google Accounts, and calculate the variation in the average visits and length of stay at different places compared to a baseline. Google provides this data for 6 categories of places: retail and recreation, grocery and pharmacy, parks, transit stations, workplace and residential. There are no further information, though, on how the measures are computed, the sample size and if it varies over time.

[11] Q&A: Similarities and differences – COVID-19 and influenza

[12] https://www.google.com/covid19/mobility/

Covid Economics 18, 15 May 2020: 1-41

Covid Economics 18, 15 May 2020: 1-41

On the other hand, the study of Pepe et al. (2020) also collects location data from users who have opted-in to provide access to their location data anonymously through agreeing to install partner apps on their smartphones. This app allows to collect geographical coordinates with an estimated accuracy level of about 10 meters. Their dataset is composed of a panel of about 167,000 users in Italy who were active during the week 22-28 February and for whom there was at least one stop collected during the same week. Individuals are then followed over the next 8 weeks. The study provides data on the average contact rate over time by constructing a proximity network between individuals, where proximity between any two users is assessed within a circle of radius 50 meters. Despite being potentially a more selected sample they compute the daily average relative degree of the network at the province level, thus providing more detailed data than Google reports.[13]

For our purposes, we have collected the average degree of the network for each of the provinces of Lombardy between 24 February and 21 March and computed a weighted average by population of each province.[14] We then compute the daily rate of change of the relative degree of the network with respect to its value on 24 February. Since after 11 March the values tend to vary little, we assume that the rate of change from the 21 March to 9 April remains unchanged.

Finally, we incorporate in our model the data on mobility obtained by these sources assuming that the rates of changes r_{mt} in mobility are proportional to the rates of changes in the average daily contact rate $\bar{n}$. In particular, assuming that p_c remains constant we have that $\beta_t = \bar{n} p_c (1 + r_{mt}) = \beta_0 (1 + r_{mt})$, which is in line with works on deterministic variation in effective daily transmission rate in SEIRD model, such as the recent Piccolomini and Zama (2020) on the Italian COVID-19 outbreak.

This alteration ultimately makes the multivariate function $\mathbf{T}_t(\boldsymbol{\alpha}_t)$ time varying. However, given that the time path of r_{mt} is completely defined beforehand, the time variation in $\mathbf{T}_t(\boldsymbol{\alpha}_t)$ is deterministic and the standard Kalman Filter equations are still valid.

3.4 Under-reporting of Cases – ϵ_t

In the same fashion as for β, we calibrate ϵ_t on the rate of change of under-reporting estimated from real data, following Villa (2020a). Specifically, let ξ_t be the adjusted daily case fatality rate of the disease, computed as the number of cumulative deaths divided by the number of cumulative official cases lagged by 6 days[15] and ι be the true infection

[13] Our analyses are robust to the use of Google mobility reports for Lombardy, too. Results are available upon request.

[14] The weighting does not have a large effect on the outcome.

[15] We choose to divide the current number of deaths by 6-day lagged cases because there is a lag between the onset of symptoms and death. The Italian Health Institute (Istituto Superiore di Sanità, ISS) quantifies this lag in a median time of 10 days. However, since there is a lag between the infection and the onset of symptoms, we rescale this factor to 6 days, following Villa (2020a).

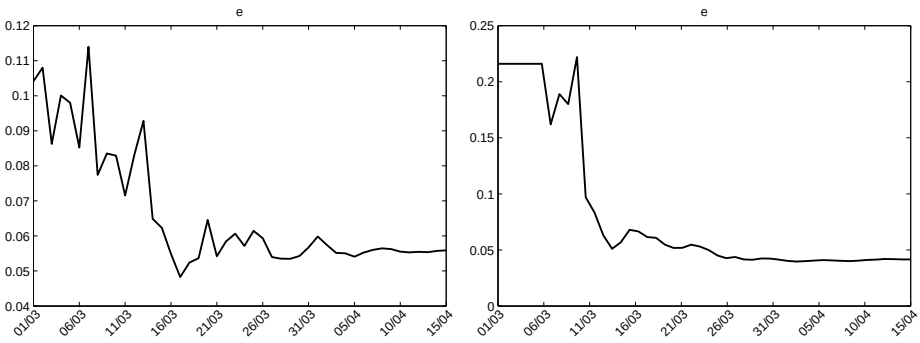

(a) Lombardy (b) London

Figure 3: Estimated values of $\tilde{\epsilon}_t$

fatality rate, which, following Ferguson et al. (2020) and Villa (2020a), is estimated to be 0.9% (95% CI: 0.4%-1.4%) for the United Kingdom and 1.14% for Italy (95% CI: 0.51%-1.78%).[16] Therefore, a proxy for ϵ_t is computed as:

$$\tilde{\epsilon}_t = \frac{\iota}{\xi_t}$$

Although the magnitude of $\tilde{\epsilon}_t$ estimated with this methodology might not exactly match the ϵ_t parameter in our SEIRD model, because of measurement error, we still believe that its variation over time might be closely related to the one that our parameter should experience if it were to be time varying. The variation in ϵ_t would represent the ability that the healthcare system has to detect infected individuals and this ability should be decreasing as the system is under stress, as we see from the results presented in Figure 3. In order to incorporate this feature, as already done for mobility, we compute the daily rate of change of $\tilde{\epsilon}_t$, $r_{\tilde{\epsilon}t}$ and we assume that $\epsilon_t = \epsilon_0 (1 + r_{\tilde{\epsilon}t})$.

3.5 Per-day Mortality Rates – γ and γ_d

We calibrate the per-day mortality rate to match the unobserved mortality computed from Istat mortality statistics for Lombardy. Specifically, we compute excess mortality as the difference between daily deaths in 2020 and average daily deaths in the previous 5 years, as in Figure 1, panel (a). The difference between excess mortality and COVID-19 official deaths represents deaths that occured in 2020 in excess relative to previous years but not officially attributed to COVID-19. Only a subset of the excess mortality in Istat data is directly or indirectly related to COVID-19. Indeed, the difference may represent: (*i*) deaths that are directly caused by COVID-19, but not reported in official statistics; (*ii*)

[16] The estimate is obtained by correcting the age-stratified infection fatality rate in Verity et al. (2020) for the demographic structure of Italy and the United Kingdom.

Covid Economics 18, 15 May 2020: 1-41

deaths for other causes indirectly related to COVID-19 (for example, if healthcare systems could not provide appropriate care to patients for other diseases because of overwhelmed hospitals); (*iii*) deaths from other causes unrelated to COVID-19. Following Bucci et al. (2020), and using one of their most conservative scenarios, we assume that only 36% of the mortality in excess to official statistics is directly related to COVID-19, but *unobserved*.[17] To this end, we set the per-day mortality rate to be $\gamma = 0.0011$. This choice ensures that we are able to match unobserved deaths in the model to the true excess mortality series, derived empirically from the data. We then assume that the per-day *detected* mortality rate is equal to three times the mortality rate for unobserved cases, i.e. $\gamma_d = 0.0033$. We make this choice, based on the fact that observed cases are generally more severe (because symptomatic) and therefore are more likely to cause complications which may result fatal.

4 The Impact of the Lockdown

4.1 Permanent Lockdown, Unmitigated Scenario and Gradual Lifting of Restrictions

Lombardy The results of our estimation are reported in Figure 4, where we assume that the restrictions in place in Lombardy remain the same until July. The top panel reports the evolution of infected, recovered and deaths in the fit window (24 February - 9 April), observed (solid lines) and unobserved (dashed lines). The middle panel reports the same set of variables, adding a forecasting window that ends in the first week of July.[18] The bottom panel reports the evolution of exposed individuals, the reproduction number R_t and the fatality rate, computed as the ratio of total deaths (observed and unobserved) over total cases, computed as the sum of infected, recovered and deaths (observed and unobserved).

The model estimates a $\hat{\beta}_0 = 0.744$ and suggests that at the end of the in-sample period there are at least twice as many infected individuals as those observed (63,202 undetected and 29,067 detected), whereas the number of recoveries is 26 times higher than those actually observed in the data: this suggests that the prevalence of the disease among the population is approximately 5.7% (computed as the sum of total recoveries and infected over the total population in Lombardy). The number of unobserved deaths – those caused by COVID-19 but unreported – is 3,470, meaning that the official death count would be underestimating the true number of deaths by as much as 35%, being the number of detected deaths 10,022. By the end of July, our model forecasts that the total number of cases is close to 1 million, the majority of which is composed of undetected recoveries.

[17] See Appendix C for a more detailed discussion on the calibration of this parameter.

[18] Figure D.1 in the Appendix plots detected infected, recovered and deaths alongside 95% bootstrapped forecasting bounds.

Covid Economics 18, 15 May 2020: 1-41

Covid Economics 18, 15 May 2020: 1-41

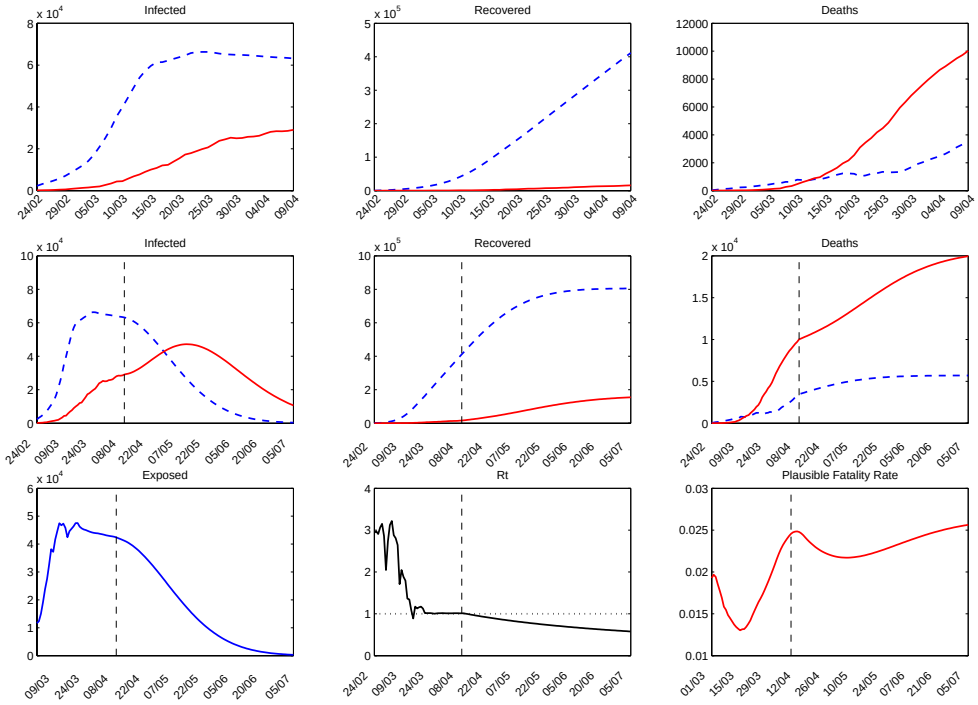

Figure 4: Baseline scenario Lombardy: permanent lockdown.

Notes. The figure shows the fitted (top panel) and forecasted (middle panel) curves of undetected (blue dashed lines) and detected (red solid lines) infections, recoveries and deaths. The bottom panel shows exposed individuals, the reproduction rate R_t and the "plausible" fatality rate. This scenario assumes that the lockdown stays in place until the end of the forecast window (5 July).

The number of observed and unobserved infected individuals fades out by the end of the forecasting period, whereas the total number of deaths equals 25 thousand, 5.7 of which unobserved.

The lockdown measures considerably reduce the number of exposed individuals, which become close to 0 by July. The reproduction rate of the disease, summarized by the variable R_t, reaches a level of 1.01 (95% CI: 0.90-1.12) by the end of the fit period and keeps decreasing until the end of the forecast window to a level of 0.58 (95% CI: 0.51-0.64).[19] The plausible fatality rate oscillates between 1.5% and 2.5% in the fit window and it stabilizes around 2-2.5% in the forecast period. Our estimate is thus in the upper bound of those found in the literature for the Italian case (Rinaldi and Paradisi, 2020; Villa et al., 2020). However, this seems plausible given the severity of the disease in the case of Lombardy and may reflect the overwhelming pressure under which the healthcare systems has been operating.

[19]Figure D.2, panel a, plots the evolution of R_t in Lombardy over time, alongside 95% bootstrapped confidence intervals, under the permanent lockdown scenario.

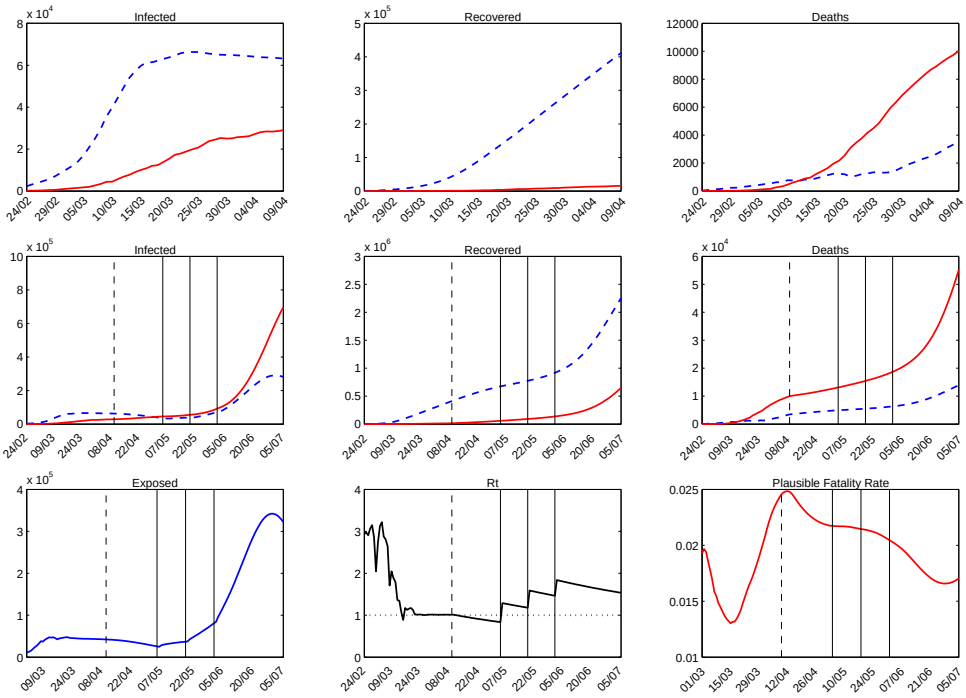

Figure 5: Current Scenario Lombardy

Notes. In this scenario, the government lifts the lockdown gradually on three dates 04/05, 18/05 and 01/06 bringing the mobility at 25%, 50% and 75% of the baseline of 24/02. The probability of contagion is unchanged.

We compare these results to a scenario where we assume that no restrictions take place, i.e. an unmitigated scenario, reported in Figure D.3. In this scenario we assume that mobility remains at the levels observed in the two weeks *before* the first cases were officially recorded in Italy.[20] In an unmitigated scenario the number of deaths is predicted to reach a level around 125,000, of which 48,000 would not be detected. The high number of undetected deaths reflects the stress under which hospitals would be put if no containment measures were adopted. The reproduction rate in this scenario fluctuates around 3.

Both these scenarios (the permanent lockdown and the unmitigated case) are only benchmarks. They show what would happen in the absence of policy interventions to lift restrictions in one case and to impose them in the other. Therefore, we also evaluate what would happen under the current policy implemented by the Italian government. Specifically, the lockdown measures have been partly lifted starting from May 4. The Italian government announced a further lifting of restrictions in the coming days, if the epidemic proves to be under control. We forecast the evolution of the epidemic under

[20]Specifically, we replicate the mobility pattern of the two weeks prior to the beginning of the epidemic until the end of the forecast window.

Covid Economics 18, 15 May 2020: 1-41

the plan of re-openings of the government under different assumptions on the evolution of mobility changes.

The current government plan entails a gradual re-opening of economic activities on three dates: May 4, May 18 and June 1. On each of these dates, we assume that mobility increases up to a fraction of its level before that any restriction was imposed. Specifically, we assume that mobility goes back to 25%, 50% and 75% of its pre-lockdown level at each subsequent date. However, we assume that the probability of contagion remains unaffected, i.e. we set p_c to be equal to its pre-lockdown level.[21] The evolution of the epidemic under this scenario, according to our model, is reported in Figure 5. The model suggests that we can expect a second peak of infections by mid-summer (middle panel of Figure 5) and a surge in deaths, both observed and unobserved. Therefore, in the current policy scenario for Lombardy, our model predicts 978,000 infected, 2.9 million recovered and 69,100 deaths, of which 280,700, 649,000 and 13,900, respectively, are undetected.

The cumulative numbers of exposed, infected, recovered and deaths under these scenarios for Lombardy are reported in Table 1, panel A, rows 1-5.

London In this case the model estimates a $\hat{\beta}_0 = 0.474$, while Figure 6 reports the forecasts of the evolution of the epidemic assuming a permanent lockdown until mid-July. Exposed individuals reach a peak in early May and then fade out, as well as infected, with a delay between detected and undetected cases. By the end of the forecast period on July 19, our model predicts a total of 13,827 detected deaths and 3,124 undetected deaths. We can compare these numbers to those that would be observed if no restrictions were imposed. Results are reported in Figure D.4. The total number of detected deaths under the no lockdown policy would reach a level of 43,754, whereas unreported deaths would be 39,295. Thus, we would observe approximately 83 thousand deaths, i.e. around 1% of the total population living in London as also measured by the case fatality rate (which in this case would coincide with the mortality rate of the disease).

The UK government has only very recently announced a plan of re-opening of economic activities, but precise dates are yet unavailable. For our purposes, we assume that the dates at which the government lifts lockdown measures are set two weeks later than Italy (i.e. on 18/05, 01/06, 15/06). We also assume, as we did for Lombardy, that on these dates mobility goes back to 25%, 50% and 75% of the baseline level. The forecasted states under this scenario are reported in Figure 7. Under this policy, the total number of deaths would be considerably reduced, even assuming that the probability of contagion remains unaffected. The cumulative number of deaths equals 23,494, whereas unobserved deaths are 5,062. The reproduction rate R_t equal 1.16 (95% CI: 1.02-1.31) at the end of the fit

[21] Since we do not have an exact measure of the average number of daily contacts among the individuals at the beginning of our sample, $\bar{n}$, we cannot disentangle p_c from β_0. However, we assume it to be close to the average of the results provided by Della Valle et al. (2007) – roughly 16 –, so that the probability of contagion estimated by our model is $p_c = 0.046$.

Covid Economics 18, 15 May 2020: 1-41

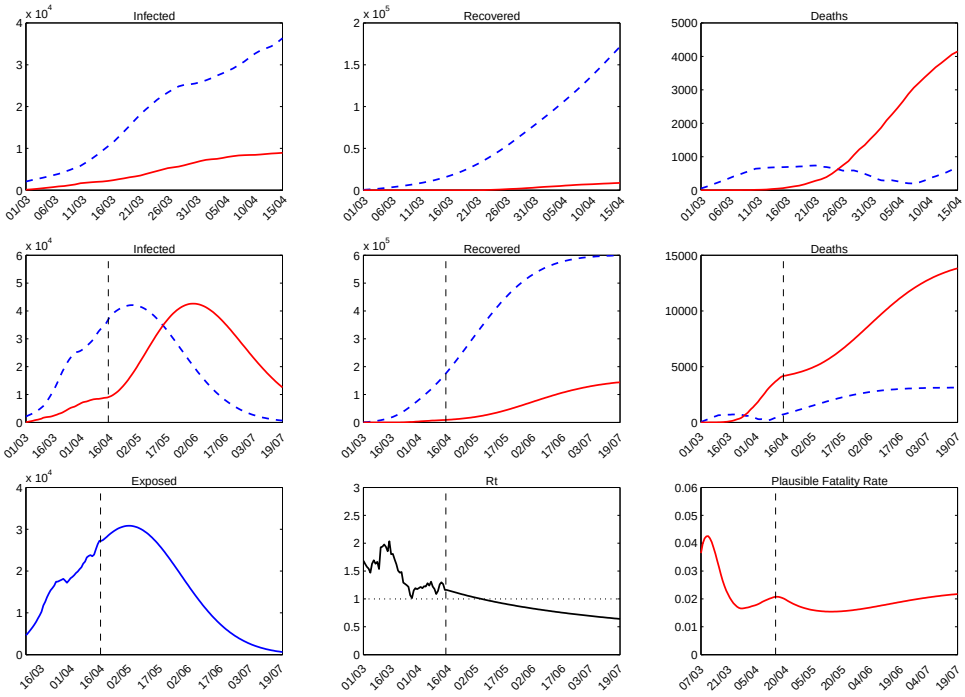

Figure 6: Baseline scenario London: permanent lockdown.

Notes. The figure shows the fitted (top panel) and forecasted (middle panel) curves of undetected (blue dashed lines) and detected (red solid lines) infections, recoveries and deaths. The bottom panel shows exposed individuals, the reproduction rate R_t and the "plausible" fatality rate. This scenario assumes that the lockdown stays in place until the end of the forecast window (19 July).

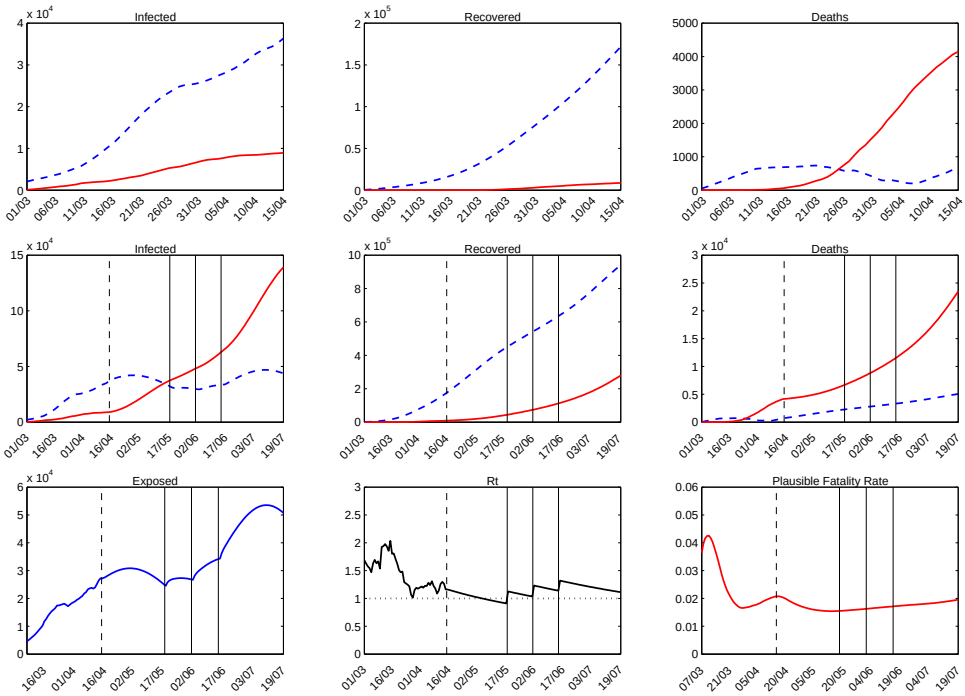

Figure 7: Current plausible scenario, London

Notes. In this scenario, the government lifts the lockdown gradually with a two weeks delay with respect to Lombardy on three dates – 18/05, 01/06 and 15/06 – bringing the mobility at 25%, 50% and 75% of the baseline of the 24/02. The probability of contagion is unchanged.

period and declines to 0.64 (95% CI: 0.56-0.72).[22]

The cumulative numbers of exposed, infected, recovered and deaths under these scenarios for London are reported in Table 1, panel B, rows 15-19.

4.2 Policy Counterfactuals

Changing mobility and opening dates We run counterfactual scenarios where we change mobility levels and dates of re-opening. Specifically, for Lombardy only,[23] we look at 5 different counterfactual policies:

1. the lockdown is gradually lifted on the three aforementioned dates, but mobility increases at 33%, 66% and 100% of its pre-lockdown level;

2. the lockdown is lifted earlier on three dates: April 27, May 11, May 25 and mobility increases at 25%, 50%, 75% of the baseline;

[22]Figure D.2, panel b, plots the evolution of R_t in London over time, alongside 95% bootstrapped confidence intervals, under the permanent lockdown scenario.

[23]Results for London are qualitatively similar and available upon request.

Covid Economics 18, 15 May 2020: 1-41

Table 1: Cumulative states at the end of fit and forecast period under different policy scenarios

		(1) E	(2) I	(3) I_d	(4) R $\times 10^3$	(5) R_d	(6) D	(7) D_d	(8) R_t	(9) R_t^{LB}	(10) R_t^{UB}
						Panel A: Lombardy					
						Fit - End date: 9 April					
1.	Baseline	42.4	63.2	29.1	411.5	15.7	3.5	10.0	1.01	0.90	1.12
2.	Unmitigated	955.2	1,804.8	493.5	5,031.3	196.8	28.5	14.1	3.36	2.99	3.73
						Forecast - End date: 5 July					
3.	Baseline	0.3	0.3	10.6	805.1	154.8	5.7	20.0	0.58	0.51	0.64
4.	Unmitigated	0.0	0.0	13.0	8,401.7	1,084.6	47.6	77.4	3.36	2.99	3.73
5.	$p_c = 100\%$	322.0	280.7	697.3	2,254.9	649.0	13.9	55.2	1.54	1.37	1.71
6.	$p_c = 90\%$	190.9	158.1	369.5	1,580.2	421.3	10.1	39.0	1.38	1.23	1.54
7.	$p_c = 80\%$	76.5	63.3	163.0	1,157.9	281.3	7.7	29.0	1.23	1.09	1.36
8.	$p_c = 70\%$	22.6	19.4	64.3	938.6	205.0	6.5	23.5	1.07	0.96	1.19
9.	$p_c = 60\%$	5.2	4.8	24.9	834.4	165.6	5.9	20.7	0.92	0.82	1.02
10.	Scenario 1	318.1	336.4	1,311.1	3,717.0	1,208.8	22.2	95.2	1.85	1.65	2.06
11.	Scenario 2	212.1	213.0	915.9	3,251.9	1,117.9	19.6	88.7	1.54	1.37	1.71
12.	Scenario 3	241.4	188.5	351.2	1,447.1	353.3	9.3	34.1	1.54	1.37	1.71
13.	Scenario 4	231.5	183.2	369.4	1,579.0	416.4	10.1	38.6	1.54	1.37	1.71
14.	Scenario 5	492.4	423.7	903.6	2,593.7	733.9	15.8	61.3	1.85	1.65	2.06
						Panel B: London					
						Fit - End date: 15 April					
15.	Baseline	27.2	36.4	8.9	171.8	8.7	0.7	4.1	1.16	1.02	1.31
16.	Unmitigated	309.5	331.6	39.4	579.4	18.6	3.3	1.3	2.23	1.95	2.51
						Forecast - End date: 19 July					
17.	Baseline	0.6	0.7	12.5	599.3	144.2	3.1	13.8	0.64	0.56	0.72
18.	Unmitigated	0.1	0.3	14.2	6,934.3	612.8	39.3	43.8	2.23	1.95	2.51
19.	$p_c = 100\%$	50.7	43.8	139.1	941.4	279.6	5.1	23.5	1.11	0.97	1.25
20.	$p_c = 90\%$	19.1	16.9	65.6	751.7	206.3	4.0	18.3	1.00	0.88	1.13
21.	$p_c = 80\%$	6.0	5.5	29.9	645.3	162.9	3.4	15.2	0.89	0.78	1.00
22.	$p_c = 70\%$	1.6	1.6	14.1	586.5	137.4	3.1	13.3	0.78	0.64	0.91
23.	$p_c = 60\%$	0.4	0.4	7.4	552.9	122.2	2.9	12.3	0.67	0.55	0.78

Notes. Columns 1-7 report the cumulative number (in thousands) of exposed (E), infected (I), detected infected (I_d), recovered (R), detected recovered (R_d), deaths (D), detected deaths (D_d). Columns 8-10 report the reproduction rate (R_t) and its 95% confidence interval (R_t^{LB} and R_t^{UB}). Panel A reports the numbers for Lombardy and panel B for London. The *Baseline* scenario assumes the presence of the lockdown until the end of the forecast period. The *Unmitigated* scenario is one where no restriction measures are taken. *Scenario 1* assumes the government gradually lifts lockdown on three dates – 04/05, 18/05, 01/06 – bringing mobility at 33%, 66% and 100% of its baseline on 24/02. *Scenario 2* anticipates the aforementioned dates by one week, whereas *Scenario 3* delays the dates by one week, both assuming mobility goes back to 25%, 50% and 75% of its baseline. *Scenario 4* and *Scenario 5* assume a slower lifting of restrictions on three dates (04/05, 25/05, 15/06) bringing mobility to 25%, 50%, 75% and 33%, 66% 100% of its baseline, respectively. The row labelled $p_c = x\%$, with $x = \{100, 90, 80, 70, 60\}$, uses the current plan of the Italian government: lifting restrictions on 04/05, 18/05, 01/06, with mobility going back to 25%, 50% and 75% of its baseline and assuming the probability of contagion is only a fraction $x\%$ of its baseline in the pre-lockdown period. For London, we assume the government lifts restrictions two weeks after Italy: 18/05, 01/06, 15/06.

Covid Economics 18, 15 May 2020: 1-41

3. the lockdown is lifted later on three dates: May 11, May 25, June 8, and mobility increases at 25%, 50%, 75% of the baseline;

4. the lockdown is lifted over a longer time horizon on three dates: May 4, May 25, June 15, and mobility increases at 25%, 50%, 75% of the baseline;

5. the lockdown is lifted over a longer time horizon on three dates: May 4, May 25, June 15, and mobility increases at 33%, 66%, 100% of the baseline;

Results for counterfactual scenarios 1-5 are reported in Figures D.5-D.9 and rows 10-14 of Table 1, panel A. The model suggests that a faster return to the mobility of the pre-lockdown period (scenario 1, Figure D.5) is associated with a second and more severe peak of the epidemic during the summer, with increases in infections and deaths, both observed and unobserved. Anticipating (scenario 2, Figure D.6) or delaying (scenario 3, Figure D.7) the lifting of restrictions has the expected effect on the number of cases: an earlier re-opening would anticipate the second peak and a later re-opening would further delay the peak. Spreading the lifting of restrictions on a longer time horizon and increasing mobility (Scenario 4 and 5, shown in Figure D.8 and D.9) makes little difference with respect to the current policy if mobility increases only up to 75% of its baseline level, but it entails more cases and deaths if mobility increases up to 100% of its baseline.

Reducing the probability of contagion p_c All these scenarios rest on the assumption that the probability of contagion remains the same throughout the whole period under analysis. However, many prevention measures will be in place and, in some cases, will be mandatory, such as, wearing masks in public, social distancing, avoid gatherings of people, higher hygienic standards, sanitizing public and private spaces. Moreover, the virus could mutate over time (although the consensus on this is not unanimous). We can nonetheless expect that "soft" containment measures reduce the probability of contagion, therefore compensating for the increased mobility. We therefore run a second set of counterfactual scenarios where we fix the dates at which the government lifts restrictions to the baseline (i.e. to the actual plan implemented by the government), but we assume different values for the probability of contagion, from 100% to 60% of its pre-lockdown levels,[24] assuming mobility increases to 25%, 50% and 75% of its pre-lockdown levels on May 4, May 18 and June 1 in Lombardy (May 17, June 1 and June 15 in London). We compare these counterfactuals to the scenario where the lockdown is maintained until the end of the period under analysis. Figures 8 and 9 show the results for detected and undetected infections and deaths in Lombardy and London, respectively.[25] The line where the probability of contagion is held constant to 1 is the same as the current policy scenario

[24]For the purpose of our model, given a deterministic path of $\bar{n}_t$, a percentage change Δ in p_c would result in an equal percentage change in β_t since $\Delta p_c \bar{n}_t \approx \Delta \beta_t$.

[25]Figure D.10 provides results for the number of exposed individuals.

Covid Economics 18, 15 May 2020: 1-41

Covid Economics 18, 15 May 2020: 1-41

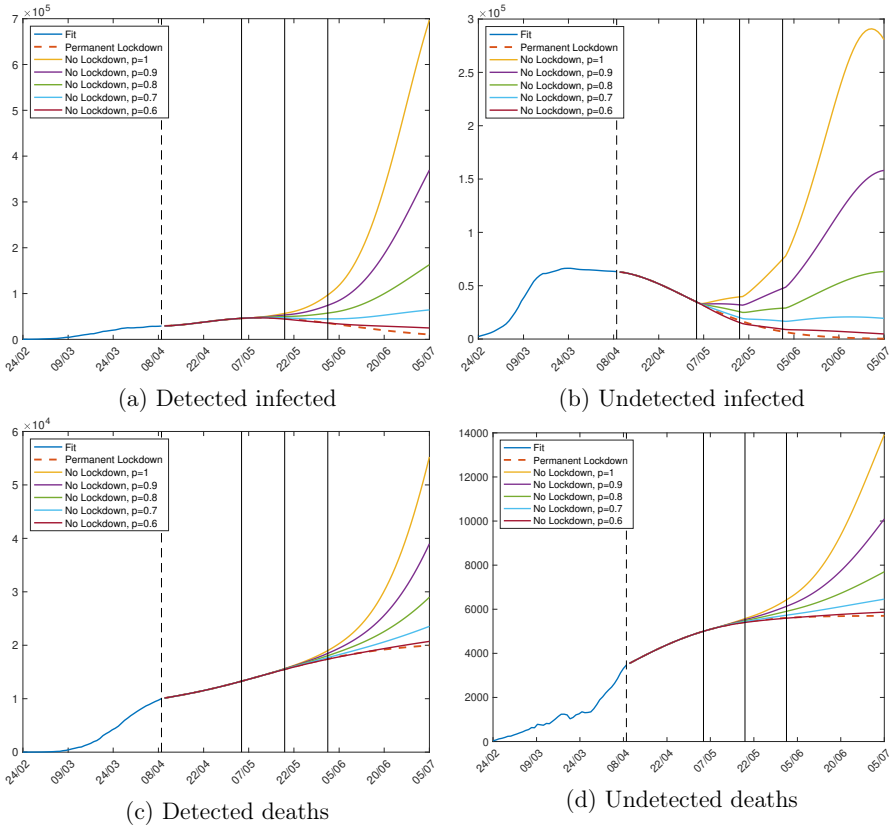

(a) Detected infected

(b) Undetected infected

(c) Detected deaths

(d) Undetected deaths

Figure 8: Detected and undetected deaths under different policy scenarios, Lombardy

Notes. The figure shows the evolution of infected and deaths under a set of counterfactual policies in Lombardy. We assume that the government lifts restrictions on three dates: 04/05, 18/05, 01/06. Vertical solid lines highlight these dates, vertical dashed line highlight the end of the fit window. On each date mobility increases at 25%, 50% and 75% of the pre-lockdown level. The counterfactuals assume different probability of contagion from 100% to 60% of its baseline. As a comparison, we also report the evolution under the permanent lockdown scenario (dashed line).

Covid Economics 18, 15 May 2020: 1-41

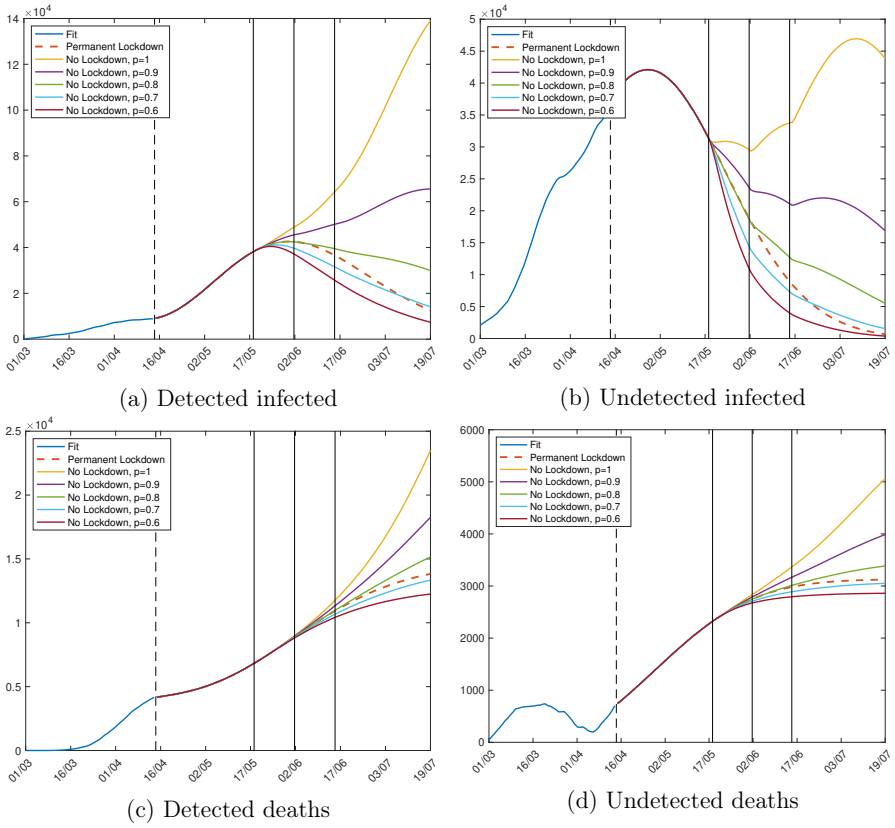

(a) Detected infected

(b) Undetected infected

(c) Detected deaths

(d) Undetected deaths

Figure 9: Detected and undetected deaths under different policy scenarios, London

Notes. The figure shows the evolution of infected and deaths under a set of counterfactual policies in London. We assume that the government lifts restrictions on three dates: 18/05, 01/06, 15/06. Vertical solid lines highlight these dates, vertical dashed line highlight the end of the fit window. On each date mobility increases at 25%, 50% and 75% of the pre-lockdown level. The counterfactuals assume different probability of contagion from 100% to 60% of its baseline. As a comparison, we also report the evolution under the permanent lockdown scenario (dashed line).

of the previous section. As highlighted already, in this scenario our model suggests that increases in mobility that are not offset by a reduced probability of contagion likely end up in a second epidemic peak. Reducing the probability of contagion makes the appearance of a second peak less likely and, as a consequence, considerably decreases the death toll. If the probability of contagion decreases at 60% of its baseline level we can expect in Lombardy a number of deaths that is very close to the permanent lockdown scenario: 20,700 detected and 5,900 undetected deaths in this counterfactual as opposed to 20,000 and 5,700, respectively, in the permanent lockdown, as shown in Table 1, row 9. In London a similar result is achieved when the probability of contagion is set between 70% and 80% of its baseline level.

Table 1 also shows that if the probability of contagion p_c does not increase to its level before the introduction of restriction measures the reproduction rate of the virus, R_t remains below 1. In the scenario where the probability of contagion is 60% of its pre-lockdown level, the forecast of R_t at the end of the forecast window is 0.92 (95% CI: 0.82-1.02) in Lombardy and 0.67 (95% CI: 0.55-0.78) in London. This evidence could provide some useful insights for policymakers when lifting restrictions and highlights the importance of adopting "soft" containment measures that could reduce the probability of infection, even when mobility goes back to its baseline levels as economic activities re-open.

5 Conclusion

This paper estimates a SEIRD epidemic model of COVID-19, by accounting for both observed and unobserved states in modeling infections, recoveries and deaths. We calibrate our model on data for Lombardy and London, two of the hardest hit regions in the world by the epidemic. We explicitly account for mobility changes due to the lockdown. We show that the under-reporting of cases and deaths is a quantitatively relevant phenomenon. Furthermore, we use the model to predict the evolution of the epidemic under different policy scenarios of lockdown lifting. We show that the lockdown has a considerable impact on total cases and deaths relative to an unmitigated scenario where the whole population would have been infected. Furthermore, we show that a gradual lifting of restrictions, in both Lombardy and London, would likely cause a second epidemic peak, which would be more severe if the return to the pre-lockdown mobility is faster. Anticipating, delaying or spreading the dates of re-opening on a longer time horizon would not change the main conclusion that a second peak is likely. However, we further show that reducing the probability of contagion to 60% of its baseline pre-lockdown level in Lombardy and between 70% and 80% in London – even in the presence of increased mobility – implies an evolution of the epidemic similar to that under a permanent lockdown scenario. Therefore, this paper provides evidence in favor of soft policies for the so called

Covid Economics 18, 15 May 2020: 1-41

"second phase," such as social distancing, wearing masks, sanitizing public and private spaces and increasing hygienic standard and, in general, all measures that can reduce the probability of infection. We see our results as a starting point, which could help policymakers in balancing the trade-off between imposing stricter measures and harming economic activity and campaigning in favor of softer measures whose efficacy ultimately depends on citizens' active collaboration. Nonetheless, more research is needed on which policy is most effective in cutting the transmission of the virus as more governments lift restrictions around the world.

References

Bucci, E., Leuzzi, L., Marinari, E., Parisi, G., and Ricci-Tersenghi, F. (2020). Un'analisi dei dati ISTAT sui decessi legati all'epidemia Covid-19 in Italia: verso una stima del numero di morti dirette ed indirette, anche grazie allo sbilanciamento di genere. Technical report, Mimeo.

Cancelli, C. and Foresti, L. (2020). The real death toll from Covid-19 is at least 4 times the official numbers. *Corriere della Sera*.

Day, M. (2020). Covid-19: four fifths of cases are asymptomatic, China figures indicate. *BMJ*, 369.

Della Valle, S., Hyman, J., Hethcote, H., and Eubank, S. (2007). Mixing patterns between age groups in social networks. *Social Networks*, 29(4):539–554.

Diekmann, O., Heesterbeek, J. A., and Metz, J. A. (1990). On the definition and the computation of the basic reproduction ratio R0 in models for infectious diseases in heterogeneous populations. *Journal of mathematical biology*, 28(4):365–382.

Doran, H. (1992). Constraining Kalman Filter and Smoothing Estimates to Satisfy Time-Varying Restrictions. *Journal of Economics and Statistics*, 74(3):568–572.

Favero, C. (2020). Why is Covid-19 mortality in Lombardy so high? Evidence from the simulation of a SEIHCR model. *Covid Economics: Vetted and Real Time Papers*, 4:47–61.

Ferguson, N., Laydon, D., Nedjati Gilani, G., Imai, N., Ainslie, K., Baguelin, M., Bhatia, S., Boonyasiri, A., Cucunuba Perez, Z., Cuomo-Dannenburg, G., et al. (2020). Report 9: Impact of non-pharmaceutical interventions (NPIs) to reduce COVID19 mortality and healthcare demand.

Covid Economics 18, 15 May 2020: 1-41

Giordano, G., Blanchini, F., Bruno, R., Colaneri, P., Filippo, A. D., and andMarta Colaneri, A. D. M. (2020). Modelling the COVID-19 epidemic and implementation of population-wide interventions in Italy. *Nature Medicine*.

Grassly, N. C. and Fraser, C. (2006). Seasonal Infectious Disease Epidemiology. *Proceedings: Biological Sciences*, 273(1600):2541–2550.

Harvey, A. (1989). *Forecasting structural time series models and the Kalman filter*. Cambridge University Press, 1 edition.

Heffernan, J. M., Smith, R. J., and Wahl, L. M. (2005). Perspectives on the basic reproductive ratio. *Journal of the Royal Society, Interface*, 2(4):281–293.

Kermack, W. O. and McKendrick, A. G. (1927). A contribution to the mathematical theory of epidemics. *Proceedings of the royal society of london. Series A, Containing papers of a mathematical and physical character*, 115(772):700–721.

Kucinskas, S. (2020). Tracking R of COVID-19. *Available at SSRN 3581633*.

Lauer, S. A., Grantz, K. H., Bi, Q., Jones, F. K., Zheng, Q., Meredith, H. R., Azman, A. S., Reich, N. G., and Lessler, J. (2020). The Incubation Period of Coronavirus Disease 2019 (COVID-19) From Publicly Reported Confirmed Cases: Estimation and Application. *Annals of Internal Medicine*, 172(9):577–582.

Lavezzo, E., Franchin, E., Ciavarella, C., Cuomo-Dannenburg, G., Barzon, L., Del Vecchio, C., Rossi, L., Manganelli, R., Loregian, A., Navarin, N., Abate, D., Sciro, M., Merigliano, S., Decanale, E., Vanuzzo, M. C., Saluzzo, F., Onelia, F., Pacenti, M., Parisi, S., Carretta, G., Donato, D., Flor, L., Cocchio, S., Masi, G., Sperduti, A., Cattarino, L., Salvador, R., Gaythorpe, K. A., Brazzale, A. R., Toppo, S., Trevisan, M., Baldo, V., Donnelly, C. A., Ferguson, N. M., Dorigatti, I., and Crisanti, A. (2020). Suppression of COVID-19 outbreak in the municipality of Vo, Italy. *medRxiv*.

Li, D., Lv, J., Botwin, G., Braun, J., Cao, W., Li, L., and McGovern, D. P. (2020a). Estimating the scale of COVID-19 Epidemic in the United States: Simulations Based on Air Traffic directly from Wuhan, China. *medRxiv*.

Li, Q., Guan, X., Wu, P., Wang, X., Zhou, L., Tong, Y., Ren, R., Leung, K. S., Lau, E. H., Wong, J. Y., Xing, X., Xiang, N., Wu, Y., Li, C., Chen, Q., Li, D., Liu, T., Zhao, J., Liu, M., Tu, W., Chen, C., Jin, L., Yang, R., Wang, Q., Zhou, S., Wang, R., Liu, H., Luo, Y., Liu, Y., Shao, G., Li, H., Tao, Z., Yang, Y., Deng, Z., Liu, B., Ma, Z., Zhang, Y., Shi, G., Lam, T. T., Wu, J. T., Gao, G. F., Cowling, B. J., Yang, B., Leung, G. M., and Feng, Z. (2020b). Early Transmission Dynamics in Wuhan, China, of Novel Coronavirus-Infected Pneumonia. *New England Journal of Medicine*, 382(13):1199–1207. PMID: 31995857.

Covid Economics 18, 15 May 2020: 1-41

Pepe, E., Bajardi, P., Gauvin, L., Privitera, F., Lake, B., Cattuto, C., and Tizzoni, M. (2020). COVID-19 outbreak response: a first assessment of mobility changes in Italy following national lockdown. *medRxiv*.

Piccolomini, E. L. and Zama, F. (2020). Preliminary analysis of covid-19 spread in italy with an adaptive seird model.

Rinaldi, G. and Paradisi, M. (2020). An empirical estimate of the infection fatality rate of COVID-19 from the first Italian outbreak. *medRxiv*.

Russo, L., Anastassopoulou, C., Tsakris, A., Bifulco, G. N., Campana, E. F., Toraldo, G., and Siettos, C. (2020). Tracing DAY-ZERO and Forecasting the Fade out of the COVID-19 Outbreak in Lombardy, Italy: A Compartmental Modelling and Numerical Optimization Approach. *medRxiv*.

Soper, H. E. (1929). The Interpretation of Periodicity in Disease Prevalence. *Journal of the Royal Statistical Society*, 92(1):34–73.

Stoffer, D. S. and Wall, K. D. (1991). Bootstrapping State-Space Models: Gaussian Maximum Likelihood Estimation and the Kalman Filter. *Journal of the American Statistical Association*, 86(416):1024–1033.

Tibayrenc, M. (2007). *Encyclopedia of Infectious Diseases: Modern Methodologies*. John Wiley & Sons, Inc., 1 edition.

Toda, A. A. (2020). Susceptible-infected-recovered (SIR) dynamics of Covid-19 and economic impact. *Covid Economics: Vetted and Real Time Papers*, 1:47–61.

Toxvaerd, F. (2020). Equilibrium Social Distancing. *Cambridge working papers in Economics No: 2020/08*.

Verity, R., Okell, L. C., Dorigatti, I., Winskill, P., Whittaker, C., Imai, N., Cuomo-Dannenburg, G., Thompson, H., Walker, P., Fu, H., Dighe, A., Griffin, J., Cori, A., Baguelin, M., Bhatia, S., Boonyasiri, A., Cucunuba, Z. M., Fitzjohn, R., Gaythorpe, K. A. M., Green, W., Hamlet, A., Hinsley, W., Laydon, D., Nedjati-Gilani, G., Riley, S., van Elsand, S., Volz, E., Wang, H., Wang, Y., Xi, X., Donnelly, C., Ghani, A., and Ferguson, N. (2020). Estimates of the severity of COVID-19 disease. *medRxiv*.

Villa, M. (2020a). Covid-19 and Italy's Case Fatality Rate: What's the Catch? Technical report, Istituto per gli Studi di Politica Internazionale.

Villa, M. (2020b). Fase 2: morti sommerse, "eccesso" di zelo? Technical report, Istituto per gli Studi di Politica Internazionale.

Covid Economics 18, 15 May 2020: 1-41

Villa, M., Myers, J. F., and Turkheimer, F. (2020). COVID-19: Recovering estimates of the infected fatality rate during an ongoing pandemic through partial data. *medRxiv*.

WHO (2020). Report of the WHO-China Joint Mission on Coronavirus Disease 2019 (COVID-19). Technical report.

Covid Economics 18, 15 May 2020: 1-41

CEPR PRESS

Appendix

A Extended Kalman Filter State Space Representation for the SEIRD Model

Our SEIRD model can be represented in non-linear state space form as

$$\mathbf{y}_t = \mathbf{Z}\boldsymbol{\alpha}_t + \boldsymbol{\varepsilon}_t \qquad \boldsymbol{\varepsilon}_t \sim N(\mathbf{0}, \Omega_\varepsilon) \tag{A.1}$$

$$\boldsymbol{\alpha}_t = \mathbf{T}(\boldsymbol{\alpha}_{t-1}) + \boldsymbol{\eta}_t \qquad \boldsymbol{\eta}_t \sim N(\mathbf{0}, \Omega_\eta) \tag{A.2}$$

where $\boldsymbol{\alpha}_t = (S_t, E_t, I_t, I_{dt}, R_t, R_{dt}, D_t, D_{dt})'$ is the unobserved state vector. The non linearity comes from the presence of multivariate vector function $\mathbf{T}(\boldsymbol{\alpha}_{t-1})$, which can be decomposed in the sum of its linear and non linear components $\mathbf{T}(\boldsymbol{\alpha}_{t-1}) = \mathbf{T} \cdot \boldsymbol{\alpha}_{t-1} + \mathbf{t}(\boldsymbol{\alpha}_{t-1})$, where

$$\mathbf{T} = \begin{pmatrix} 1 & 0 & 0 & 0 & 0 & 0 & 0 & 0 \\ 0 & (1-\sigma) & 0 & 0 & 0 & 0 & 0 & 0 \\ 0 & \sigma & (1-\epsilon-\delta-\gamma) & 0 & 0 & 0 & 0 & 0 \\ 0 & 0 & \epsilon & (1-\delta_d-\gamma_d) & 0 & 0 & 0 & 0 \\ 0 & 0 & \delta & 0 & 1 & 0 & 0 & 0 \\ 0 & 0 & 0 & \delta_d & 0 & 1 & 0 & 0 \\ 0 & 0 & \gamma & 0 & 0 & 0 & 1 & 0 \\ 0 & 0 & 0 & \gamma_d & 0 & 0 & 0 & 1 \end{pmatrix}$$

$$\mathbf{t}(\boldsymbol{\alpha}_{t-1}) = \begin{pmatrix} -\frac{\beta}{N-D_{t-1}-D_{dt-1}} S_{t-1} I_{t-1} \\ \frac{\beta}{N-D_{t-1}-D_{dt-1}} S_{t-1} I_{t-1} \\ \mathbf{0}_{6\times 1} \end{pmatrix}$$

Following Harvey (1989) the approximate Extended Kalman Filter can be applied to a non-linear state space model approximating $\mathbf{T}(\boldsymbol{\alpha}_{t-1})$ through its Tailor Expansion as $\mathbf{T}(\boldsymbol{\alpha}_{t-1}) \simeq \mathbf{T}(\hat{\boldsymbol{a}}_{t-1}) + \hat{\mathbf{T}} \cdot (\boldsymbol{\alpha}_{t-1} - \hat{\boldsymbol{a}}_{t-1})$, where $\hat{\boldsymbol{a}}_{t-1}$ is the updated state vector obtained from the updating recursions of the Kalman Filter and $\hat{\mathbf{T}} = \mathbf{T} + \hat{\mathbf{t}}$, where

Covid Economics 18, 15 May 2020: 1-41

$$\hat{\mathbf{t}} = \left.\frac{\partial \mathbf{t}\left(\boldsymbol{\alpha}_{t-1}\right)}{\partial \boldsymbol{\alpha}_{t-1}'}\right|_{\boldsymbol{\alpha}_{t-1}=\hat{\boldsymbol{a}}_{t-1}} =$$

$$= \begin{pmatrix} -\hat{I}_{t-1} & 0 & -\hat{S}_{t-1} & 0 & 0 & 0 & -\frac{\beta}{\left(N-\hat{D}_{t-1}-\hat{D}_{dt-1}\right)}\hat{S}_{t-1}\hat{I}_{t-1} & -\frac{\beta}{\left(N-\hat{D}_{t-1}-\hat{D}_{dt-1}\right)}\hat{S}_{t-1}\hat{I}_{t-1} \\ \hat{I}_{t-1} & 0 & \hat{S}_{t-1} & 0 & 0 & 0 & \frac{\beta}{\left(N-\hat{D}_{t-1}-\hat{D}_{dt-1}\right)}\hat{S}_{t-1}\hat{I}_{t-1} & \frac{\beta}{\left(N-\hat{D}_{t-1}-\hat{D}_{dt-1}\right)}\hat{S}_{t-1}\hat{I}_{t-1} \\ & & & & & & \mathbf{0}_{6\times 8} & \end{pmatrix} \times$$

$$\times \frac{\beta}{\left(N-\hat{D}_{t-1}-\hat{D}_{dt-1}\right)}$$

Here $\hat{S}_{t-1}$, $\hat{I}_{t-1}$, $\hat{D}_{t-1}$ and $\hat{D}_{dt-1}$ are the updated quantities obtained form the updated vector $\hat{\boldsymbol{a}}_{t-1}$.

Then the state equation (A.2) can be rewritten as

$$\boldsymbol{\alpha}_t = \left(\mathbf{t}\left(\boldsymbol{a}_{t-1}\right) - \hat{\mathbf{t}} \cdot \boldsymbol{a}_{t-1}\right) + \hat{\mathbf{T}} \cdot \boldsymbol{\alpha}_{t-1} + \boldsymbol{\eta}_t$$

Covid Economics 18, 15 May 2020: 1-41

Covid Economics 18, 15 May 2020: 1-41

B Derivation of R_0

Following Diekmann et al. (1990), the R_0 of our SEIRD model can be computed from the leading eigenvalue of the Next Generation Matrix. In our model, we have three states that describe the dynamics between the infected and non infected individuals, E_t, I_t and I_{dt}. The first difference of these three states reads as follows

$$\begin{aligned}
\Delta E_t &= -\sigma E_{t-1} + \frac{\beta}{N - D_{t-1} - D_{dt-1}} S_{t-1} I_{t-1} \\
\Delta I_t &= -\left(\delta + \epsilon + \gamma\right) I_{t-1} + \sigma E_{t-1} \\
\Delta I_{dt} &= -\left(\delta_d + \gamma_d\right) I_{dt-1} + \epsilon I_{t-1}
\end{aligned}$$

Then we need to identify the vectors $\mathcal{F}$ and $\mathcal{V}$ at the steady state of the system, which are the terms describing respectively the evolution of the new infections from the susceptible equation and the outflows from the infectious states. At the steady state we have that $S^* = N - D^* - D_d^*$, then

$$\mathcal{F} = \begin{pmatrix} \beta I^* \\ 0 \\ 0 \end{pmatrix} \qquad \mathcal{V} = \begin{pmatrix} \sigma E^* \\ \left(\epsilon + \delta + \gamma\right) I^* - \sigma E^* \\ \left(\delta_d + \gamma_d\right) I_d^* - \epsilon I^* \end{pmatrix}$$

From this we can compute their Jacobian matrices with respect to the exposed and infected states

$$F = \nabla \mathcal{F} = \begin{pmatrix} 0 & \beta & 0 \\ 0 & 0 & 0 \\ 0 & 0 & 0 \end{pmatrix} \qquad V = \nabla \mathcal{V} = \begin{pmatrix} \sigma & 0 & 0 \\ -\sigma & \left(\epsilon + \delta + \gamma\right) & 0 \\ 0 & -\epsilon & \left(\delta_d + \gamma_d\right) \end{pmatrix}$$

The Next Generation Matrix is the product FV^{-1} which describes the expected number of secondary infections in compartment i produced by individuals initially in state j. In our case we have

$$FV^{-1} = \begin{pmatrix} \frac{\beta}{\epsilon+\delta+\gamma} & \frac{\beta}{\epsilon+\delta+\gamma} & 0 \\ 0 & 0 & 0 \\ 0 & 0 & 0 \end{pmatrix}$$

From this we can compute the dominant eigenvalue (or spectral radius) from the characteristic equation of its eigendecomposition

$$\left|FV^{-1} - \lambda I_3\right| = \lambda^2 \left(\frac{\beta}{\epsilon + \delta + \gamma} - \lambda\right) = 0$$

which has two repeated solutions at $\lambda = 0$ and one at

$$\lambda = \frac{\beta}{\epsilon + \delta + \gamma}$$

which is our R_0.

Covid Economics 18, 15 May 2020: 1-41

CEPR PRESS

Covid Economics 18, 15 May 2020: 1-41

C Calibration of the Per-day Mortality Rate γ

As highlighted in the main text, we calibrate the per-day mortality rate γ so to estimate a number of unobserved deaths that equals a fraction of the excess mortality calculated from Istat data. Specifically, Bucci et al. (2020) exploit the gender unbalance in the number of deaths to decompose the excess mortality observed in Istat statistics into: deaths directly caused by COVID-19, but unreported in official data; deaths indirectly linked to COVID-19 (because of the pressure on hospitals at the peak of the epidemic); deaths unrelated to COVID-19. They provide estimates for various Italian regions and provinces and, among them, Lombardy. They show that, under different assumptions about the gender-specific mortality rate of COVID-19, the fraction of unreported deaths can range between 16% and 57% of the excess mortality with respect to the official death toll.[1] We therefore calibrate γ in order for our model to estimate a number of unobserved deaths that is equal to the simple average of these values, i.e. 36%. We find that $\gamma = 0.0011$ provides a series that resembles closely the cumulative deaths from Istat data, rescaled by this factor, as shown in Figure C.1.

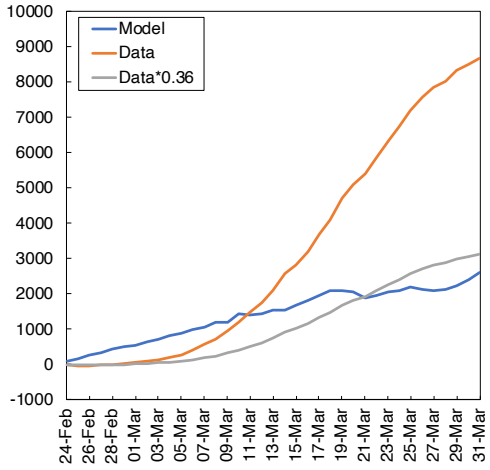

Figure C.1: Unobserved deaths, model and data

Notes. The figure reports the cumulative unobserved deaths from the SEIRD model and the excess mortality from Istat death registries, computed as the excess mortality in 2020 relative to the average of previous 5 years *minus* the official COVID-19 death toll. The latter is shown in levels and scaled by a factor of 0.36, following Bucci et al. (2020).

We also assume that the observed per-day mortality rate is three times larger than the unobserved one, i.e. $\gamma_c = 0.0033$, based on the fact the detected infections are usually symptomatic and more severe cases that are more likely to end up in critical conditions. The same parameters are used also when estimating the model on data for London.

[1] They also provide an estimate where the number of undetected deaths is higher than those detected, but we deem this as an extreme scenario.

D Additional Figures

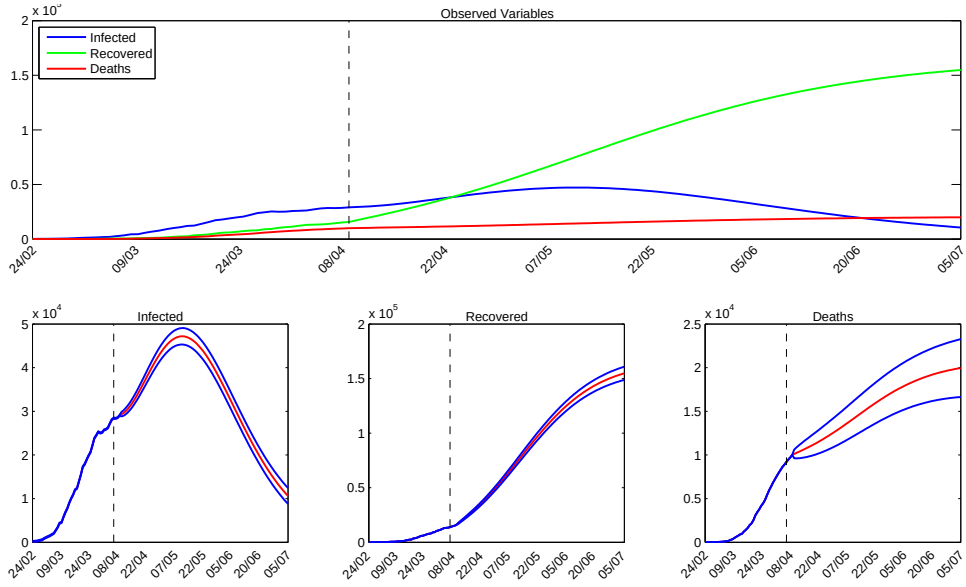

Figure D.1: Baseline scenario Lombardy: permanent lockdown.

Notes. The top panel shows fitted values and forecasts of detected infections, recoveries and deaths. The bottom panel shows the same quantities, alongside the inefficient 95% forecasting confidence bounds.

Covid Economics 18, 15 May 2020: 1-41

Covid Economics 18, 15 May 2020: 1-41

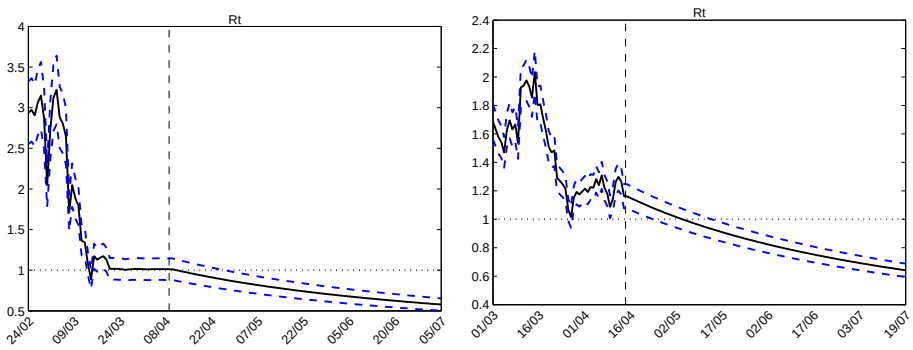

(a) Lombardy (b) London

Figure D.2: Estimated and forecast values of R_t in the baseline scenario of permanent lockdown, with the 95% bootstrapped confidence intervals.

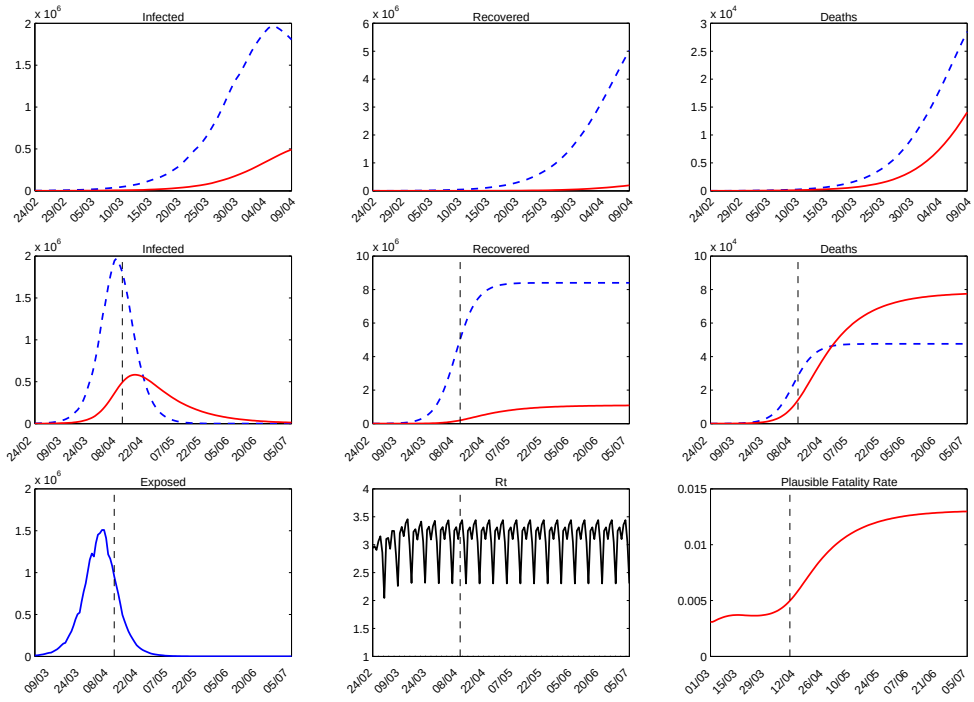

Figure D.3: Worst case scenario Lombardy: no lockdown.

Covid Economics 18, 15 May 2020: 1-41

Covid Economics 18, 15 May 2020: 1-41

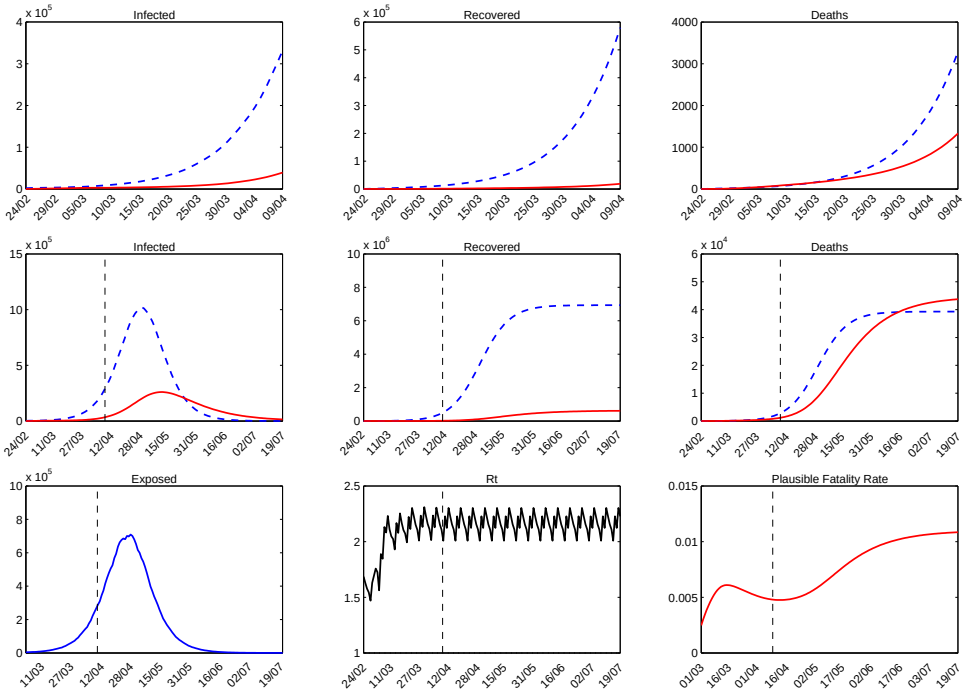

Figure D.4: Worst case scenario London: no lockdown.

Covid Economics 18, 15 May 2020: 1-41

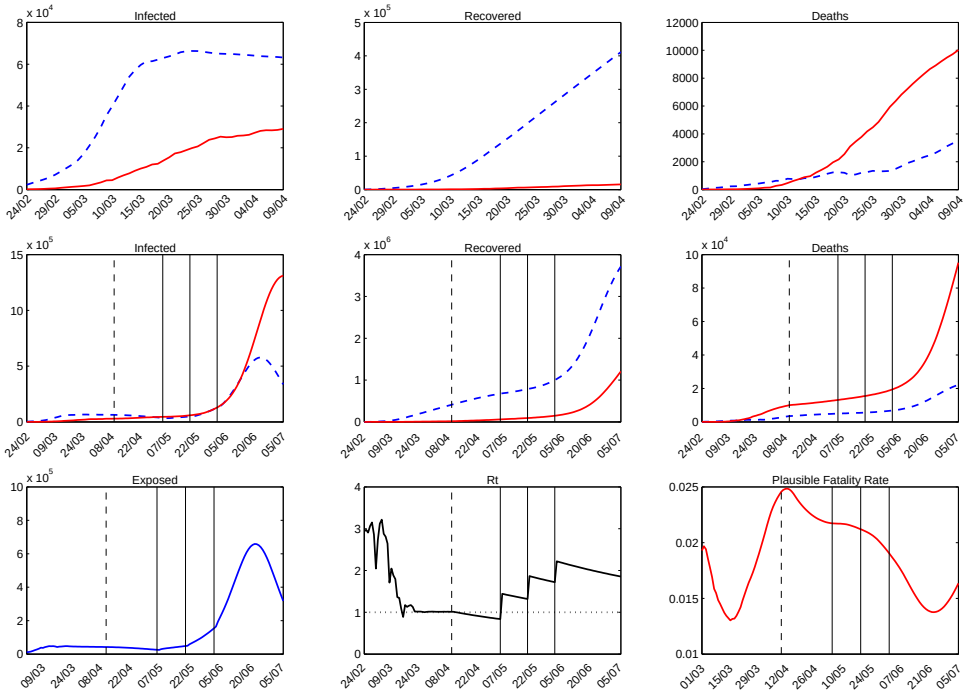

Figure D.5: Counterfactual scenario 1, Lombardy

Notes. In this scenario, the government lifts the lockdown gradually on 04/05, 18/05 and 01/06 bringing the mobility at 33%, 66% and 100% of the baseline of the 24/02.

Covid Economics 18, 15 May 2020: 1-41

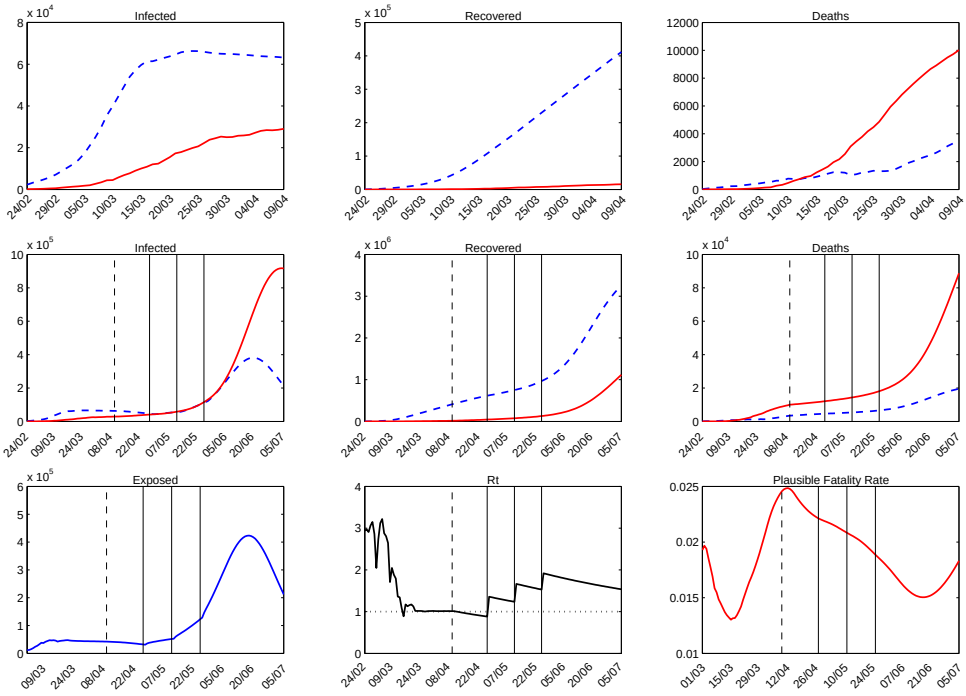

Figure D.6: Counterfactual scenario 2, Lombardy

Notes. In this scenario, the government lifts the lockdown gradually early on 27/04, 11/05 and 25/05, bringing the mobility at 25%, 50% and 75% of the baseline of the 24/02.

Covid Economics 18, 15 May 2020: 1-41

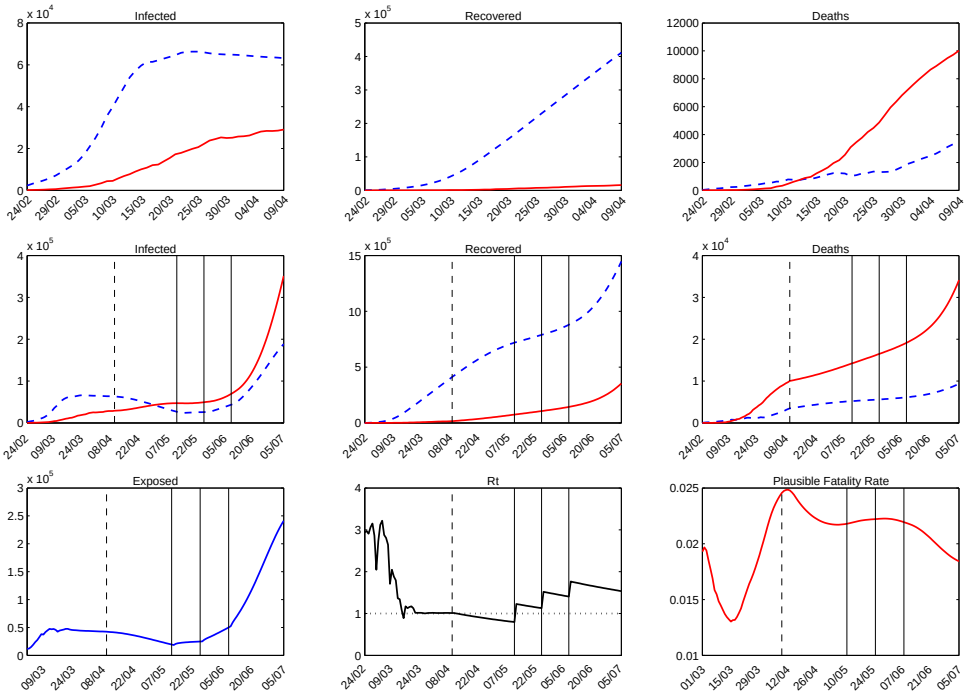

Figure D.7: Counterfactual scenario 3, Lombardy

Notes. In this scenario, the government lifts the lockdown gradually later on three dates 11/05, 25/05 and 08/06 bringing the mobility at 25%, 50% and 75% of the baseline of the 24/02.

Covid Economics 18, 15 May 2020: 1-41

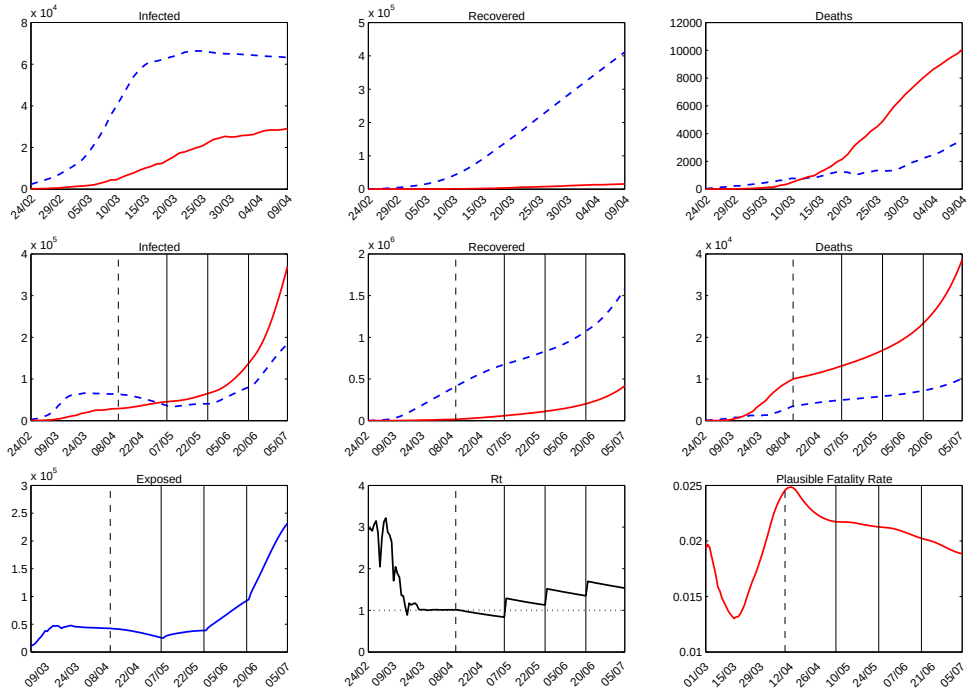

Figure D.8: Counterfactual scenario 4, Lombardy

Notes. In this scenario, the government lifts the lockdown gradually later on three dates 04/05, 25/05 and 15/06 bringing the mobility at 25%, 50% and 75% of the baseline of the 24/02.

Covid Economics 18, 15 May 2020: 1-41

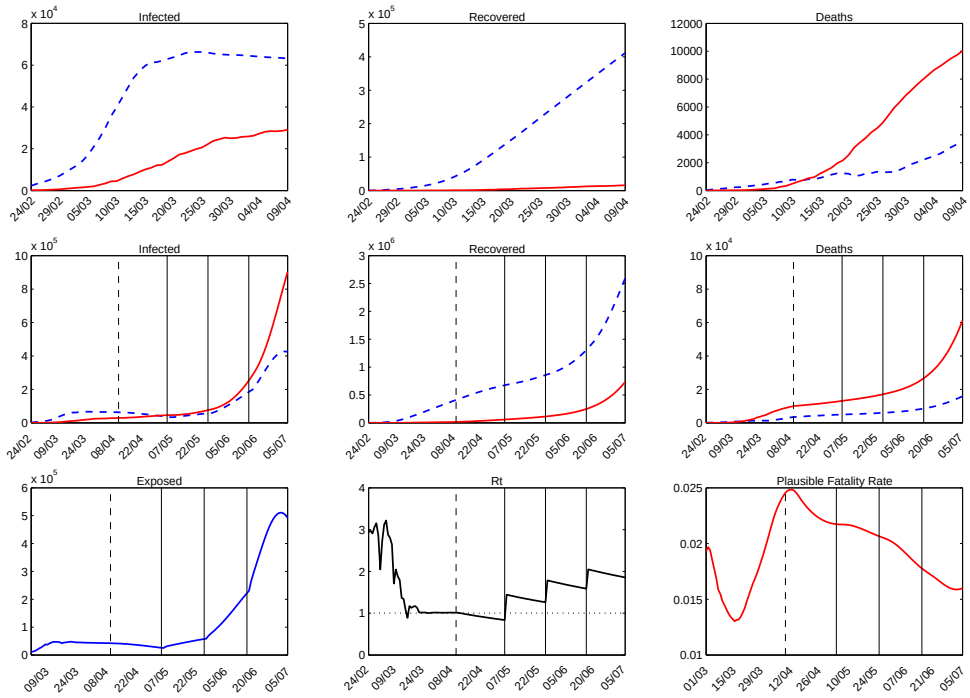

Figure D.9: Counterfactual scenario 5, Lombardy

Notes. In this scenario, the government lifts the lockdown gradually later on three dates 11/05, 25/05 and 08/06 bringing the mobility at 33%, 66% and 100% of the baseline of the 24/02.

Covid Economics 18, 15 May 2020: 1-41

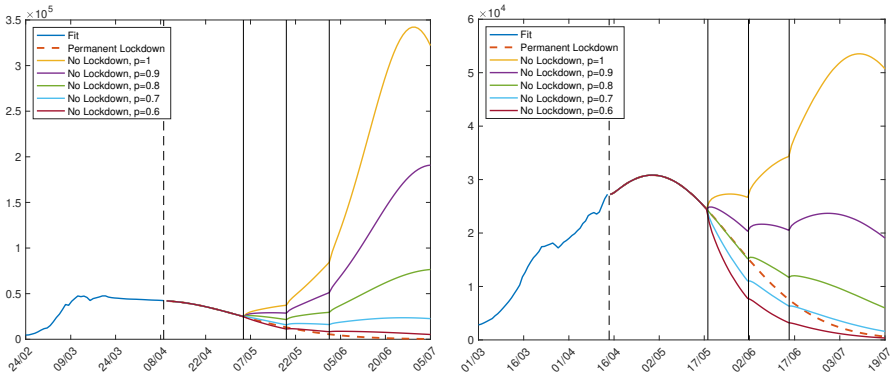

(a) Exposed, Lombardy (b) Exposed, London

Figure D.10: Exposed individuals in Lombardy and London under different probabilities of contagion

Notes. The figure shows the evolution of exposed individuals under a set of counterfactual policies in Lombardy (panel a) and London (panel b). We assume that the government lifts restrictions on three dates: 04/05, 18/05, 01/06 in Lombardy and 18/05, 01/06 and 15/06 in London. Vertical solid lines highlight these dates, vertical dashed line highlight the end of the fit window. On each date mobility increases at 25%, 50% and 75% of the pre-lockdown level. The counterfactuals assume different probability of contagion from 100% to 60%. As a comparison, we also report the evolution under the permanent lockdown scenario (dashed line).